

Deep learning based enhancement of ordered statistics decoding of LDPC codes

Guangwen Li, Xiao Yu

Abstract—Aiming at designing plausible decoders with channel information free, low complexity, high throughput, and approaching maximum likelihood performance, we put forward a streamlined architecture which concatenates sequentially three components. Specifically, to tackle the decoding failures of normalized min-sum, the whole decoding trajectory, not limited to the last iteration information conventionally, is fed into a trained convolutional neural network to yield new reliability metric for each sequence bit, termed decoding information aggregation. Then an adapted order statistics decoding, following the suggested decoding path, is adopted to process the sequence ordered with new metric more efficiently in that many invalid searches contained in conventional methods otherwise are evaded. The role of decoding information aggregation is elaborated via statistics data to reveal that it can arrange more error-prone bits into the fore part of most reliable basis of order statistics decoding, which is vital for the effective decoding enhancement. We argue the superposition of improved bitwise reliability of the most reliable basis and the imposed rigorous code structure by OSD enables the proposed architecture being a competitive rival of the state of the art decoders, which was verified in extensive simulation in terms of performance, complexity and latency for short and moderate LDPC codes.

Index Terms—Deep learning, Neural network, Belief propagation, Min-Sum, Training

I. INTRODUCTION

The channel coding is an indispensable ingredient in telecommunication system to ensure reliable information transmission. Among the vast family of linear block codes, categorized as one important class of channel coding schemes, the low-density parity-check codes (LDPC) [1] has demonstrated its pronounced error correction capability by approaching Shannon Limit asymptotically [2]. For those LDPC codes of short to moderate lengths, typically encountered in the applications such as Internet of Things (IOT) where the requirement of low complexity and low latency is stringent, standard iterative belief propagation (BP) decoder may give its way to its approximation such as min-sum (MS) variants [3], [4] for the sake of limited computational resources. Compared with the optimal most likelihood (ML) decoding, BP is sub-optimal for LDPC codes of finite length due to the existence of short cycles in code structure, and the simplified MS versions worsen the situation further in terms of performance. Therefore, a lot of attention is directed on bridging the non-negligible performance gap.

The ordered statistics decoder (OSD) was proposed [5] to approximate the ML decoder for short linear block codes at the expense of endurable complexity increase. Then as a postprocessing procedure, it was suggested and verified [6], [7] to invoke OSD to deal with the decoding failures every a few BP iterations for the LDPC codes. However, the decoding throughput is evidently suppressed in virtue of such a configuration. Since the OSD implementation is a serial block in essence, while the iterations of BP can be highly parallelizable, the interleaving of BP and OSD will result in a mismatch of processing capacity between them. For the purpose of accelerating decoding speed or reducing OSD complexity, [8] derived two early stopping criteria to threshold the predefined conditions, equipped with a devised probabilistic measure for all candidate codewords and latent error patterns, and their effectiveness was justified via simulation results on BCH codes. Likewise, [9] attempted diminishing OSD overhead by stipulating two preconditions for calling in binary Gaussian elimination (GE) operation, and it was found the savings of GE workload is substantial at high signal noise ratio (SNR) region with little performance penalty.

On the other hand, the emerged omnipotent deep learning paradigm sheds light on the feasible transfer from domains of image processing [10], natural language processing [11], challenging autonomous driving [12] etc. to the realm of error correction coding. For the task of designing a powerful neural networking (NN) decoding architecture, the seminal work of Nachmani et al. [13] suggested to unroll the standard BP into a specific NN after weighting each message edge, in the hope of circumventing the phenomenon of 'the curse of dimensionality' in code space [14], which may occur when confronted with a NN without any prior structure. To avoid the complexity of involved \tanh or inverse \tanh functions in standard BP, the NN version of normalized min-sum (NMS) [3] and offset min-sum (OMS) decoders [4], in the form of convolutional neural network (CNN) or recurrent neural network (RNN), was reported to be capable of achieving leading decoding performance for classical block codes [15]–[20]. Interestingly, a senior NN with the role of a teacher, was instructed to guide the new one toward the direction of better decoding via training [21]. In [22], a NN, created to distill out these unimportant check nodes belonging to the overcomplete parity-check matrix H in each layer, can reach a good trade-off of performance and complexity for short LDPC codes. But it is challenging to secure a qualified overcomplete H with an increase of code length. In [23], with the assistance of a NN to decide which variable node to decimate, a neural BP with

G.Li is with the College of Information & Electronics, Shandong Technology and Business University, Yantai, China e-mail: lgwa@sdu.edu.cn

X.Yu is with the Department of Physical Sports, Binzhou Medical University, Yantai, China e-mail: yuxiao@bzmu.edu.cn

decimation (NBP-D), ensembling multiple decoding results, was able to boost decoding performance remarkably, but at the cost of high complexity. Catered for these BP decoding failures which are due to some dominant absorbing sets in the LDPC code structure, a handful of RNN models were designed [24] and trained respectively for each type of the absorbing sets, and it was found the combination of BP-RNN ensemble and OSD can approach ML performance fairly close for short LDPC codes, hence regarded as the state of the art (SOTA) decoder. However, an effective training of this scheme requires great efforts to be taken and its scalability to longer codes remains to be clarified.

With the goal of seeking a decoder of unified architecture which bring together the merits of low complexity, high throughput, and quasi-SOTA performance, plus the attributes of no request of prior channel knowledge, the auto-adaptiveness in a wide range of SNR region and easy-training, we propose to merge sequentially the NMS and a revised OSD, with a trained NN inserted between them to optimize bit reliability metric. Considering the parallel processing of NMS will leave behind only a few decoding failures for the serial processing of succeeded OSD, the processing mismatch can be largely relieved with respect to latency, which underlies the selection of our architecture. The main contributions of this paper consist of,

- * For reliability metric of each NMS decoding failure, different from the substitution with magnitude of receiving sequence or a posteriori values of last decoding iteration, a synthesized alternative, or output of a simple CNN fed with the whole decoding trajectory of each decoding failure bit, is proposed to replace the conventional ones. Such a process, termed decoding information aggregation (DIA), proved to be fundamental in the sense it not only boosts the subsequent OSD enormously, but also benefits any OSD variants introduced in the literature.
- * For conventional order- p OSD implementation with respect to most reliable basis (MRB) of parity check matrix \mathbf{H} , at most p erroneous bits are assumed in the MRB, it was found much of the traversing through all possible positions of MRB is invalid or inefficient due to the exhausting search, which aggravates the computation or memory requirement. We propose to segment the MRB, and to allocate the OSD a fixed decoding path composed of dominant order patterns, which are derived from the counts statistics of erroneous bits in each segment with highest frequency. The OSD, imposed with such a tailored processing priority, proved to be effective by saving most parts of the workload of conventional routine.
- * For short codes, the proposed NMS-DIA-OSD architecture was validated to be comparable to the SOTA decoder in terms of decoding performance, and have an edge over the latter in terms of complexity, latency, training easiness etc.. Furthermore, we extended our method into high rate LDPC codes of block length over 1000, and found it could approach the ML curve within 0.35 dB at

the expense of moderate computational complexity, not reported by its counterparts.

The rest of the paper is organized as follows. Section II presents the necessary preliminaries about BP decoding variants and OSD variants. The motivation of our work is elaborated in Section III, while the decoding performance of simulation results and complexity analysis are demonstrated in Section IV. Section V concludes this paper with some remarks and suggestions of further research.

II. PRELIMINARIES

Given a binary row message vector $\mathbf{m} = [m_i]_1^K$, the encoder transforms it into $\mathbf{c} = [c_i]_1^N$ by calling $\mathbf{c} = \mathbf{m}\mathbf{G}$ in $GF(2)$, where K and N are the length of message and codeword respectively, and the generator matrix \mathbf{G} is assumed full-rank without loss of generality.

After the simple binary phase shift keying (BPSK) modulation maps each codeword bit c_i into one symbol by $s_i = 1 - 2c_i$, a sequence $\mathbf{y} = [y_i]_1^N$ with $y_i = s_i + n_i$ is received at the channel output, where n_i denotes the channel noise of mean zero and variance σ^2 . With the definition of log-likelihood ratio (LLR) of the i -th bit as

$$l_i = \log \left(\frac{p(y_i|c_i = 0)}{p(y_i|c_i = 1)} \right) = \frac{2y_i}{\sigma^2} \quad (1)$$

it is seen the magnitude of y_i is a sound metric to measure how reliable the i -th bit is. Larger magnitude implies more confidence of its hard decision \hat{c}_i being '1' or '0', depending on the sign of y_i . Namely, $\hat{c}_i = \mathbf{1}(y_i < 0)$, where $\mathbf{1}(\cdot)$ is the indicator function.

A. Standard BP and MS variants

The bipartite Tanner graph of a code, whose structure pertains totally to its \mathbf{H} , consists of N variable nodes and M check nodes, as well as the edges connecting variable node i and check node j , indicative of each '1' at the i -th row and j -th column of \mathbf{H} .

For LDPC codes, the standard BP is a competitive one among many decoding schemes, in the sense it is optimal under the assumption of a tree-like Tanner graph without any cycles. However, for any code of finite length, it degrades into a suboptimal decoder, due to the existing short cycles in the Tanner graph impairs the independence requirement of communicated messages.

To be self-contained, let us take a close look at the flooding message schedule of BP. Assume $t \in \{1, 2, \dots, T\}$, where T is the maximum number of iterations, the message from variable node v_i to check node c_j at the t -th iteration is 2

$$x_{v_i \rightarrow c_j}^{(t)} = l_i + \sum_{\substack{c_p \rightarrow v_i \\ p \in \mathcal{C}(i)/j}} x_{c_p \rightarrow v_i}^{(t-1)} \quad (2)$$

while the reversed message from c_j to v_i is 3

$$x_{c_j \rightarrow v_i}^{(t)} = 2 \tanh^{-1} \left(\prod_{\substack{v_q \rightarrow c_j \\ q \in \mathcal{V}(j)/i}} \tanh \left(\frac{x_{v_q \rightarrow c_j}^{(t)}}{2} \right) \right) \quad (3)$$

where $\mathcal{C}(i)/j$ denotes all neighboring check nodes of v_i excluding c_j , and $\mathcal{V}(j)/i$ denotes all neighboring variable nodes of c_j excluding v_i .

Thus the a posteriori value of the i -th bit at the t -th iteration, whose sign determines its hard decision, is

$$x_{v_i}^{(t)} = l_i + \sum_{\substack{c_p \rightarrow v_i \\ p \in \mathcal{C}(i)}} x_{c_p \rightarrow v_i}^{(t-1)} \quad (4)$$

To reduce intensive computation, a simple approximation (5) is substituted for the computation of \tanh or \tanh^{-1} functions in (3) for the MS algorithm, at the price of some performance loss.

$$x_{c_j \rightarrow v_i}^{(t)} = s_{c_j \rightarrow v_i}^{(t)} \cdot \omega_{c_j \rightarrow v_i}^{(t)} \quad (5)$$

where

$$s_{c_j \rightarrow v_i}^{(t)} = \prod_{\substack{v_q \rightarrow c_j \\ q \in \mathcal{V}(j)/i}} \text{sgn} \left(x_{v_q \rightarrow c_j}^{(t)} \right)$$

and

$$\omega_{c_j \rightarrow v_i}^{(t)} = \min_{\substack{v_q \rightarrow c_j \\ q \in \mathcal{V}(j)/i}} \left| x_{v_q \rightarrow c_j}^{(t)} \right|$$

What makes the MS more attractive is its characteristic of scale invariance to channel noise. As opposed to it, standard BP will suffer seriously from inaccurate estimation of σ^2 [18].

To narrow the performance gap between MS and BP decoders, the NMS or OMS were proposed to weight or offset appropriately the min term in (5).

On the other hand, traditional BP, NMS or OMS can be readily transformed into a trellis structure by unrolling each iteration of its decoding process respectively, subjected to the extra complexity by imposing weights or offsets on the neural networking edges. Among the NN versions of BP, NMS, and OMS, with the fact BP possesses the highest complexity, and OMS generally lags behind NMS [18] in terms of performance, we prefer the NMS version in its simplest form. Namely, the NN whose edges incidental to the min term in 5 are all weighted with a shared parameter across iterations.

In training phase, neural decoder is fed with a batch of data, then evaluated for the output with the routine cross-entropy loss function. Then a stochastic gradient descent (SGD) optimizer is called to update the single parameter. The training process repeats till a stopping criteria is triggered. It is found that a well trained NMS can compensate for most performance loss between the MS and BP.

B. Two classes of OSD variants

Roughly, all OSD variants can be categorized into two classes.

For one, all binary operations evolve around \mathbf{G} . Specifically, after all bits of a received sequence are sorted in descending order according to the reliability metric, it is divided into two sections, among which the MRB is composed of the first K bits of the sorted list and the least reliable basis (LRB) includes the rest of the bits.

After the GE operation solicited on \mathbf{G} , we abridge the result as

$$\tilde{\mathbf{c}} = [\tilde{\mathbf{c}}_1 : \tilde{\mathbf{c}}_2] = \tilde{\mathbf{m}} \tilde{\mathbf{G}} = \tilde{\mathbf{m}} [\mathbf{I} : \mathbf{P}] = [\tilde{\mathbf{m}} : \tilde{\mathbf{m}} \mathbf{P}] \quad (6)$$

condensed from

$$(\mathbf{c} \mathbf{G}_{c_1} \mathbf{G}_{c_2}) = (\mathbf{m} \mathbf{G}_{r_2}^{-1}) (\mathbf{G}_{r_2} \mathbf{G} \mathbf{G}_{c_1} \mathbf{G}_{c_2}) \quad (7)$$

where \mathbf{G}_{c_1} denotes the requested column swaps of \mathbf{G} due to bit reliability ordering, and \mathbf{G}_{r_2} , \mathbf{G}_{c_2} stand for equivalent row and column operations when reducing \mathbf{G} of full row rank into its systematic form. Notably, the operation attributed to \mathbf{G}_{c_2} may cause sorting order to be disrupted locally. Based on the assumption that most received bits keep their authentic signs even under disturbed transmission, the order- p OSD infers that $\bar{\mathbf{c}}_1$ of $[\bar{\mathbf{c}}_1 : \bar{\mathbf{c}}_2] = \hat{\mathbf{c}} \mathbf{G}_{c_1} \mathbf{G}_{c_2}$, subjected to at most p positions, is a good approximation of its MRB, implied by $\tilde{\mathbf{c}}_1 = \tilde{\mathbf{m}}$ in 6, where $\hat{\mathbf{c}} = [\hat{c}_i]_1^N$ is the hard-decision of $[y_i]_1^N$. Next, within a Hamming distance p of centered around the known $\bar{\mathbf{c}}_1$, we list all possible estimates for the authentic MRB $\tilde{\mathbf{c}}$ by appealing to error pattern $\mathbf{e}_j = [e_i]_1^K$ with at most p nonzero bits in it, $j \in \sum_{\delta=0}^p \binom{K}{\delta}$, then $\bar{\mathbf{c}}_{1j} = \bar{\mathbf{c}}_1 \oplus \mathbf{e}_j$, as the j -th estimate of $\tilde{\mathbf{m}}$, when multiplied by \mathbf{P} , will yield $\bar{\mathbf{c}}_{2,j}$ as an estimate of authentic LRB as implied in 6. Lastly, all reconstructed candidate codewords, in the form of $\bar{\mathbf{c}}_j = [\bar{\mathbf{c}}_{1j} : \bar{\mathbf{c}}_{2j}] = [\hat{c}_i]_1^N$, compete for the best estimate of $\tilde{\mathbf{c}}$ under the criterion of

$$\tilde{\mathbf{c}} = \arg \min_{\bar{\mathbf{c}}_j = [\hat{c}_i]_1^N} \sum_{i=1}^N \mathbf{1}(\hat{c}_i \neq \tilde{c}_i) |y_i| \quad (8)$$

For another, as a duality of above mentioned, the objective is to reduce \mathbf{H} via GE operation. analogous to 6 and 7, we have

$$\mathbf{H} \mathbf{c}^T = \mathbf{0} \Rightarrow \tilde{\mathbf{H}} \tilde{\mathbf{c}}^T = [\mathbf{I} : \mathbf{Q}] [\tilde{\mathbf{c}}_1 : \tilde{\mathbf{c}}_2]^T = \mathbf{0} \quad (9)$$

from

$$(\mathbf{H}_{r_2} \mathbf{H} \mathbf{H}_{c_1} \mathbf{H}_{c_2}) (\mathbf{H}_{c_2}^{-1} \mathbf{H}_{c_1}^{-1} \mathbf{c}^T) = \mathbf{0} \quad (10)$$

where \mathbf{H}_{c_1} is the equivalent matrix for reordering $[y_i]_1^N$ in ascending order, then \mathbf{H}_{r_2} and \mathbf{H}_{c_2} , equivalent to row and column operations on \mathbf{H} , further transform \mathbf{H} into the form $[\mathbf{I} : \mathbf{Q}]$, among which the left submatrix is an identity matrix. Since $\bar{\mathbf{c}}_2$ of $\bar{\mathbf{c}} = [\bar{\mathbf{c}}_1 : \bar{\mathbf{c}}_2]$, as the hard decision of reordered $[y_i]_1^N$ relating to $\mathbf{H}_{c_1,2}$, is mapped to the MRB bits, then the binary sum of $\bar{\mathbf{c}}_2$ and each error pattern \mathbf{e}_j with order at most p , denoted as $\bar{\mathbf{c}}_{2,j}$, is a qualified estimate of authentic $\bar{\mathbf{c}}_2$. Hence, it can be substituted for $\bar{\mathbf{c}}_2$ in 9 to calculate the estimate $\bar{\mathbf{c}}_{1j}$ of another authentic part $\bar{\mathbf{c}}_1$, thus one valid candidate

codeword $\bar{c}_j = [\bar{c}_{1j}, \bar{c}_{2j}]$ is induced. Lastly, the most likely codeword can be chosen among all the candidates under the same criterion of 8.

III. MOTIVATIONS

A. Rationale of DIA

The power of OSD depends largely on choosing K qualified ones among all the bits of a sequence to fill the MRB, where as fewer as possible erroneous bits is expected to be included. Therefore, the problem of how to construct an exceptional MRB reduces to seeking a new reliability metric which decides the barriers to entry of MRB. Conventionally, the reliability of each sequence bit is measured by its magnitude manifested in the last NMS decoding iteration. However, considering the NMS decoder leaves behind a posterior probability value of each bit per decoding iteration, which actually evolves around the underlying ground truth, even for the cases of decoding failure, hence there is a good odds to configure a better estimate of the authentic via aggregating information from the whole iterative decoding trajectory, instead of drawing on the last iteration only.

To this end, we resort to deep learning based CNN for its properties of quick response and high abstraction ability. Specifically, a posteriori value of each bit at each decoding iteration makes up a unique time series, the length of which is T . Then after flowing it through a CNN created by a number of off-shelf Conv1D layers of keras package on Tensorflow platform, we can obtain a synthesized reliability metric for the referred bit.

B. Architecture of NMS-DIA-OSD

In our configuration, NMS can process the received sequences in batch, and the decoding trajectory of its decoding failures, is merged via DIA to generate new metric for each bit, which will be subsequently directed to OSD as inputs to enhance its decoding.

The merit of such an arrangement is that the limited sequential processing capacity of OSD with a small amount of input data matches the parallelizable NMS implementation fed with volumes of data to the greatest extent, thus enabling this architecture to exhibit higher throughput and less latency. The block-diagram of it is shown in 1.

C. Adapted OSD algorithm

Hereafter, we focus on the description of the second class of OSD evolving around \mathbf{H} . Even with the assistance of DIA, the essential process of reducing \mathbf{H} into its systematic form, may push some bits used to belonging to LRB to be exchanged into the MRB field, raising the risk of containing more erroneous bits in the latter.

To combat it, we suggest to segment the MRB unevenly into 3 parts, where the leftmost, called low reliable zone (LRZ), is reserved mainly for those bits exchanged from LRB field, the middle one is a buffer called medium reliable zone (MRZ), and the rightmost part called high reliable zone (HRZ), set aside for the most reliable bits, will occupy most space of

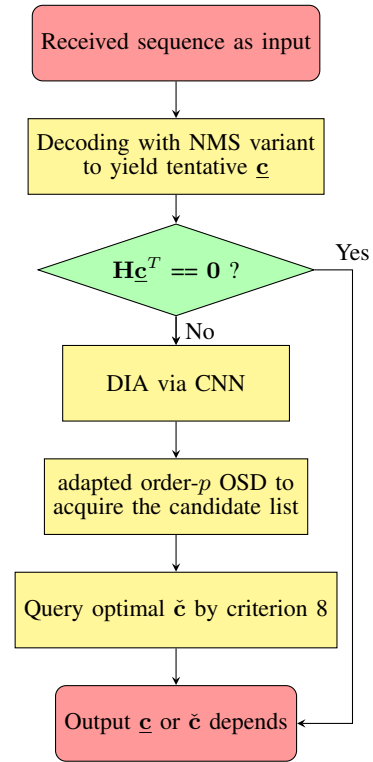


Fig. 1. Flowchart of NMS-DIA-OSD architecture

the whole MRB. Next, a tuple termed order pattern, recording the counts of erroneous bits in three segments, is labeled as dominant or not depending on its occurrences in the simulation at a typical SNR point. Such a layout admits more erroneous bits occur in the left two parts than the third one, for the sake of curbing complexity while missing as little as possible authentic error patterns. Then all the dominant order patterns constitute a decoding path, along which the OSD starts off its decoding. Meanwhile, the components of the decoding path can be trimmed or skipped depending on performance requirement or complexity restriction, thanks to the decoding and complexity of the OSD adhering to the decoding path is now highly predictable.

The pseudo-code of our adapted OSD is detailed in Alg. 1. In sum, the LRB bits go through twice ordering, one based on the new reliability metric, one due to GE operation, while the MRB bits request an extra ordering to fix the order disruption originated from GE. Another modification occurs at step 5,6 which relates to the operations of decoding path. Notably, the 'repeat' block and last step of finding the optima can be parallelized by populating a tensor and calling in tensor operations efficiently.

IV. SIMULATION RESULTS AND COMPLEXITY ANALYSIS

Owing to space limitations, we focus only on two classes of LDPC codes: One is the short half rate CCSDS LDPC (128,64) code [20] [25], shortened as Code A. Another is a longer WiMAX (802.16) (1056,880) code with rate 5/6 [20], shortened as Code B. All simulations are carried out

Algorithm 1 Adapted decoding path based OSD algorithm

Input: new reliability metric of each sequence bit from DIA, and a predetermined decoding path of length P_d

Output: optimal codeword estimate \check{c}

- 1: $[\hat{y}_i]_1^N$ is the sorted results from $[y_i]_1^N$ in ascending order of its magnitude measured by new reliability metric, and $\hat{\mathbf{H}}$ corresponds to the result of \mathbf{H} after due column swaps \mathbf{H}_{c_1} , namely, $\hat{\mathbf{H}} = \mathbf{H}\mathbf{H}_{c_1}$
- 2: $\hat{\mathbf{H}}$ is reduced into its systematic form $\mathbf{H}_s = [\mathbf{I} : \mathbf{Q}]$ via Gaussian elimination, namely, $\mathbf{H}_s = \mathbf{H}_{r_2} \hat{\mathbf{H}} \mathbf{H}_{c_2} \mathbf{H}_{c_3}$, with \mathbf{H}_{c_3} equivalent to the functionality of keeping the MRB bits in strict ascending order.
- 3: Impacted by the due column swaps $\mathbf{H}_{c_2} \mathbf{H}_{c_3}$, $[\hat{y}_i]_1^N$ is the sorted results from $[\hat{y}_i]_1^N$, yielding the MRB baseline $\check{c}_2 = [\check{c}_i]_{N-K+1}^N$, where $\check{c}_i = \mathbf{1}(\hat{y}_i < 0)$.
- 4: **for** $l \in \{0, 1, 2, \dots, P_d\}$ **do**
- 5: **repeat:**
- 6: Generate an error pattern \mathbf{e}_j qualified for the l -th order pattern, and $\mathbf{e}_j \oplus \check{c}_2 \Rightarrow \check{c}_{2j}$, $\check{c}_{1j} = \mathbf{Q}\check{c}_{2j}$
- 7: Append new generated codeword $\check{c}_j = [\check{c}_{1j} : \check{c}_{2j}]$ into the candidate codeword list
- 8: **until** traversing ends
- 9: **end for**
- 10: **return** optimal \check{c} among above list under criterion 8

on Tensorflow platform of Google, and the source code can be retrieved in github at a later time.

A. Distribution of MRB order

For a NMS decoding failure, the number of erroneous bits in its MRB is defined as MRB order conventionally. It is meaningful to compare the distribution of MRB order to identify the effect of DIA involvement. For Code A, at two typical SNR points of 2.8 dB and 3.5 dB in the waterfall region, we calculated the relative frequency by recording counts of MRB order in terms of the conventional metric and new metric respectively, or named 'pre' and 'pro' in the legend of Fig. 2 and 3, with their cumulative distribution function (CDF) curves illustrated as well. It is observed the low MRB order cases account for most of decoding failures for both metrics. For instance, at SNR=2.8 dB, the ratio of order-0,1 cases approximates 0.87 and 0.95 separately. When SNR is shifted to 3.5 dB, the ratio is also lifted to 0.93 and 0.98 respectively. Furthermore, whatever 2.8 or 3.5 dB, the observation that the CDF attached to new metric consistently prevails over the conventional one, exhibits the involvement of DIA can effectively reduce the number of erroneous bits in the MRB, which implies better OSD decoding improvement given a specific order. For longer Code B, a similar observation holds as well. Simultaneously, drawn from Table I, we found the number of categories related to the MRB order shrinks whenever DIA is involved. For instance, it drops from 17 to 10 at 3.2 dB, and from 7 to 6 at 3.6 dB for Code B. Beyond

that, the heavy tail phenomenon is greatly relieved in the case of DIA assistance.

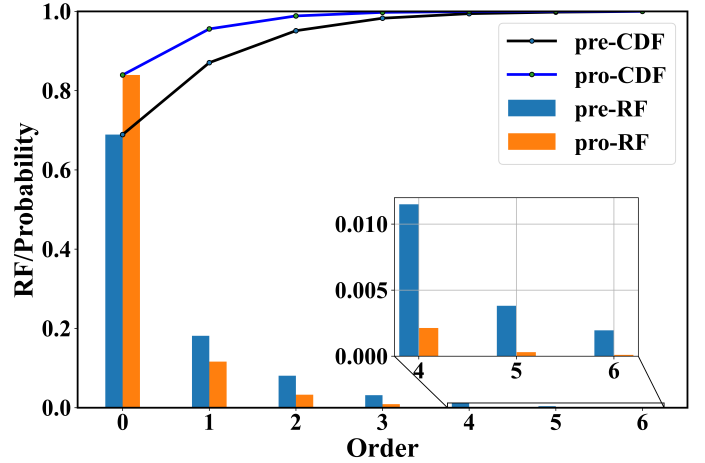


Fig. 2. Distribution of MRB order for NMS decoding failures of (128,64) code at the point SNR=2.8 dB w/o DIA

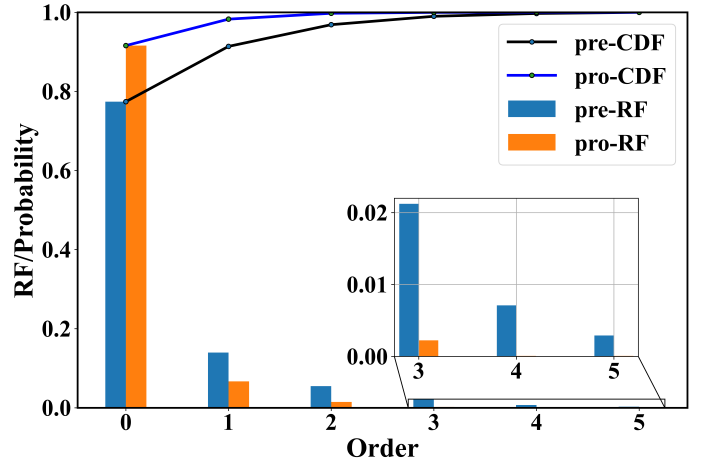


Fig. 3. Distribution of MRB order for NMS decoding failures of (128,64) code at the point SNR=3.5 dB w/o DIA

TABLE I
COUNTS OF MRB ORDER FOR NMS DECODING FAILURES W(IN BOLD)/WO DIA

Codes	SNR(dB)	Counts
(128,64)	2.8	0: 27086, 1: 7130, 2: 3169, 3: 1240, 4: 452, 5: 150, 6: 60, 7: 14, 8: 2, 9: 1 0: 32997 , 1: 4567 , 2: 1287 , 3: 353 , 4: 84 , 5: 12 , 6: 3 , 7: 1
	3.5	0: 10356, 1: 1870, 2: 734, 3: 284, 4: 95, 5: 25, 6: 9, 7: 3, 8: 1, 9: 1 0: 12253 , 1: 895 , 2: 198 , 3: 30 , 4: 1 , 5: 1
(1056,880)	3.2	0: 6276, 1: 2944, 2: 2039, 3: 1371, 4: 872, 5: 541, 6: 327, 7: 186, 8: 108, 9: 77, 10: 38, 11: 26, 12: 11, 13: 5, 14: 10, 15: 2, 16: 1, 18: 1 0: 8778 , 1: 2950 , 2: 1525 , 3: 800 , 4: 408 , 5: 204 , 6: 95 , 7: 36 , 8: 18 , 9: 15 , 10: 6
	3.6	0: 316, 1: 84, 2: 60, 3: 30, 4: 19, 5: 5, 6: 3, 7: 5 0: 419 , 1: 72 , 2: 15 , 3: 9 , 4: 4 , 5: 1 , 6: 2

B. Distribution of swap counts

Considering the swaps requested when reducing the $\hat{\mathbf{H}}$ further into its systematic form is the root cause to break strict

ordering of MRB bits with respect to some reliable metric, thus the bits related to the swaps, when entering the MRB field, are the least reliable compared with other bits of the MRB. Let n_{sw} denote the number of swaps between tentative MRB and LRB, then it is sensible to query its distribution due to it is a baseline to guide us to determine the length of three MRB zones. Beyond that, the segmentation of MRB will indirectly impact the decoding path selection.

As illustrated in Fig. 4, average $n_{sw} = 4$ for Code A, no sensitive to SNR = 2.8 or 3.5 dB. As a comparison, for longer Code B, average n_{sw} will soar to 44, indicating more bits used to belonging to LRB have to be placed in the LRZ of MRB, For one thing, it is beneficial to accommodate more failure cases in an enlarged LRZ. For another, we have to restrict LRZ size so as to manage well the resulting complexity. Therefore, we have to make a compromise as for the LRZ scope. With reference to the distribution n_{sw} , the segmentation of MRB is delimited at two points 20, 40 for Code A, and 40,120 for Code B in the following simulations. Additionally, no obvious discrepancy between CDF curves of Code A at 2.8 and 3.5 dB implies similar complexity on average for a decoding failure at any SNR point.

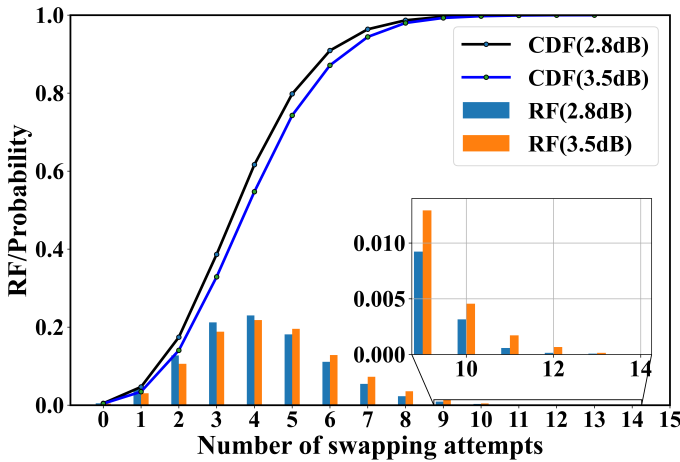


Fig. 4. Distribution of number of swapping attempts between MRB and LRB regions when reducing $\widehat{\mathbf{H}}$ into systematic form for NMS decoding failures of (128,64) code at the point SNR=2.8, 3.5dB

C. Dominant order pattern of OSD

For any code, its MRB is segmented into LRZ, MRZ and HRZ, whose length is respectively λ_1 , λ_2 and λ_3 with the sum being K. Correspondingly for the l -th link along the decoding path, a specific order pattern $[a^{(l)}, b^{(l)}, c^{(l)}]$ denotes the set whose elements are these binary error patterns having $a^{(l)}, b^{(l)}, c^{(l)}$ non-zeros in three zones sequentially, what intrigues us most is the distribution of dominant order pattern which occurred most frequently.

For Code A, we list the first 20 dominant order patterns with and without DIA in Table II. Evidently, it shows more decoding failures are categorized into fewer dominant order

patterns with the aid of DIA. At 3.0 dB, when imposing the requirement of order sum $a^{(l)} + b^{(l)} + c^{(l)} < 5$, then the decoding failures have the probability of $(33795 - 3)/33807 = 0.9995$ being trapped by the first 20 dominant order patterns when equipped with DIA. In contrast to it, the probability drops to $(33517 - 35)/33807 = 0.9904$ without DIA. Then based on the counts of these dominant order patterns, and with curbing complexity in mind, it is natural to choose the first 19 dominant order patterns to compose the optimal decoding path when P_l is set 19 with the existence of DIA. In comparison, the first 20 dominant ones (except next-to-last) constitute the optimal decoding path without DIA. Then after checking the elements of two decoding paths mentioned, we found they are almost the same up to some inner permutations among these dominant order patterns. Furthermore, when the tested SNR point is shifted up or down, or P_l varies due to applications, the decoding path commonly alters little, which ensures the decoding path once chosen is universal in the sense it is almost optimal across a wide range of SNR region of interest. When compared the discrepancy of decoding path between Code A and B, it is found the leading order patterns mostly overlaps, hinting the cross-code possibility of the chosen decoding path.

For longer Code B at 3.5 dB, as shown in Table II, decoding failures scatter onto more order patterns. Though P_l is relaxed from 20 to 32, the dominant order patterns cover only a ratio of $6135/6199 = 0.9896$ of all decoding failures with DIA, and in comparison it degrades to $5684/6199 = 0.9169$ without DIA, all under the condition of order sum $a^l + b^l + c^l < 6$. Obviously, such a dispersiveness causes the computing resources required to enhance the performance of longer codes to soar dramatically. Therefore, to curb the total complexity in practice, the dominant order patterns with high order sum may be trimmed from the decoding path at the expense of sacrificing a certain amount of performance.

Given a decoding path, we can either predict precisely the possible decoding performance, or equivalently, it is feasible to evaluate how many computing resources are required to attain a targeted decoding performance.

TABLE II
COUNTS OF THE FIRST 20 AND 32 DOMINANT ORDER PATTERNS FOR NMS-(DIA)-OSD OF CODE A AND B RESPECTIVELY

SNR(# of cases)	Conditions	Patterns/Counts & sum
Code A 3.0 dB (33807)	without DIA	$['[0\ 0\ 0]', '[1\ 0\ 0]', '[2\ 0\ 0]', '[0\ 1\ 0]', '[1\ 1\ 0]', '[2\ 1\ 0]', '[3\ 0\ 0]', '[0\ 0\ 1]', '[1\ 0\ 1]', '[1\ 2\ 0]', '[0\ 2\ 0]', '[3\ 1\ 0]', '[2\ 0\ 1]', '[4\ 0\ 0]', '[2\ 2\ 0]', '[0\ 1\ 1]', '[1\ 1\ 1]', '[2\ 1\ 1]', '[3\ 2\ 0]', '[3\ 0\ 1]']$ [22950, 4865, 1506, 1175, 901, 419, 391, 201, 166, 163, 132, 123, 94, 85, 82, 81, 79, 40, 35, 29] & 33517
	with DIA	$['[0\ 0\ 0]', '[1\ 0\ 0]', '[0\ 1\ 0]', '[2\ 0\ 0]', '[1\ 1\ 0]', '[3\ 0\ 0]', '[0\ 0\ 1]', '[2\ 1\ 0]', '[1\ 0\ 1]', '[0\ 2\ 0]', '[1\ 2\ 0]', '[3\ 1\ 1]', '[3\ 0\ 1]', '[1\ 1\ 1]', '[2\ 0\ 1]', '[4\ 0\ 0]', '[2\ 2\ 0]', '[0\ 3\ 0]', '[1\ 2\ 1]', '[5\ 0\ 0]']$ [27729, 3910, 727, 666, 304, 110, 99, 65, 41, 38, 25, 16, 12, 11, 11, 10, 9, 5, 4, 3] & 33795
Code B 3.5 dB (6199)	without DIA	$['[0\ 0\ 0]', '[1\ 0\ 0]', '[0\ 1\ 0]', '[1\ 1\ 0]', '[2\ 0\ 0]', '[2\ 1\ 0]', '[1\ 0\ 1]', '[1\ 0\ 1]', '[0\ 2\ 0]', '[1\ 2\ 0]', '[3\ 0\ 0]', '[1\ 1\ 1]', '[0\ 1\ 1]', '[2\ 0\ 1]', '[3\ 1\ 0]', '[2\ 1\ 1]', '[2\ 2\ 0]', '[2\ 2\ 1]', '[1\ 1\ 2]', '[0\ 2\ 1]', '[3\ 1\ 1]', '[3\ 0\ 1]', '[1\ 2\ 1]', '[3\ 2\ 0]', '[1\ 0\ 2]', '[0\ 1\ 2]', '[4\ 0\ 0]', '[1\ 3\ 0]', '[4\ 1\ 1]', '[0\ 3\ 0]', '[1\ 2\ 2]', '[0\ 0\ 2]']$ [2466, 789, 353, 305, 267, 152, 134, 120, 95, 91, 86, 78, 78, 72, 62, 59, 51, 35, 34, 34, 34, 32, 32, 30, 28, 27, 26, 25, 24, 23, 22, 20] & 5684
	with DIA	$['[0\ 0\ 0]', '[1\ 0\ 0]', '[0\ 1\ 0]', '[2\ 0\ 0]', '[1\ 1\ 0]', '[0\ 0\ 1]', '[1\ 0\ 1]', '[2\ 1\ 0]', '[0\ 2\ 0]', '[1\ 0\ 1]', '[3\ 0\ 0]', '[1\ 2\ 0]', '[2\ 0\ 1]', '[3\ 1\ 0]', '[0\ 2\ 1]', '[0\ 3\ 0]', '[0\ 0\ 2]', '[2\ 1\ 1]', '[1\ 2\ 1]', '[3\ 0\ 1]', '[1\ 0\ 2]', '[1\ 1\ 2]', '[1\ 1\ 2]', '[3\ 2\ 0]', '[2\ 3\ 0]', '[0\ 3\ 1]', '[5\ 0\ 0]', '[4\ 1\ 0]', '[4\ 0\ 0]']$ [3217, 1082, 440, 269, 244, 135, 98, 89, 85, 63, 60, 52, 46, 27, 27, 27, 24, 22, 20, 13, 13, 11, 11, 9, 9, 9, 6, 6, 6, 5, 5, 5] & 6135

D. Decoding performance

The success of NMS-DIA-OSD depends largely on the close collaboration of triple constituent phases. Generally speaking, NMS outputs the trajectory of decoding failures to DIA, then the latter generates a more reliable metric as the input of OSD, which then start off post-processing according to the preset decoding path identified by previous simulations at a typical SNR point.

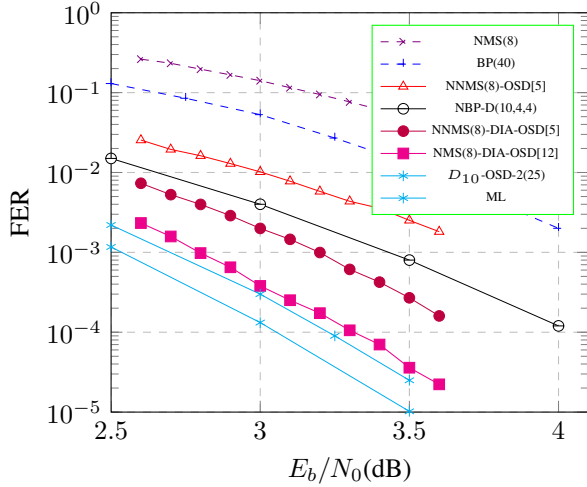


Fig. 5. FER comparison for various decoding schemes of (128,64) code

For Code A, we adhere to the decoding path directed by Table II at 3.0 dB. Fig.5 presents various FER results under the condition of varied decoding path length P_l , in addition to the cases of with or without DIA. For comparison purpose, the FER performance of NMS, BP, a competitive decoder 'NBP-D(10,4,4)' from [23], a SOTA decoder ' D_{10} -OSD-2' from [24], as well as ML decoding [26], are included. In the legend list, the maximum iteration number I_m of decoders is in parentheses and P_l in square brackets. Since I_m impacts the succeeded layout of CNN layers, besides the decoding performance of NMS itself, it is our motivation to keep I_m confine as small as a small number such as 8 to mitigate computational complexity of the class of NMS-DIA-OSD.

As depicted in Fig.5, low-complexity NMS lags behind conventional BP decoding of $I_m = 40$ with no surprise, but it surpasses the latter considerably when concatenated with OSD of $P_l = 5$. Furthermore, with the aid of DIA, namely, the conventional reliability metric is replaced by the synthesized output of trained CNN, another performance gain of at least 0.5 dB is observed, which excels the NBP-D(10,4,4), about 0.3 dB at FER = 10^{-4} . When P_l expands to 12, we found the FER curve of 'NMS(8)-DIA-OSD[12]' is boosted to be within 0.3 dB of ML in the waterfall region, manifesting itself as a serious competitor to the SOTA decoder of D_{10} -OSD-2 by exhibiting a slightly inferior decoding performance. Obviously, if more computing resources are committed into growing P_l , it is expected to be the rival of any leading decoders.

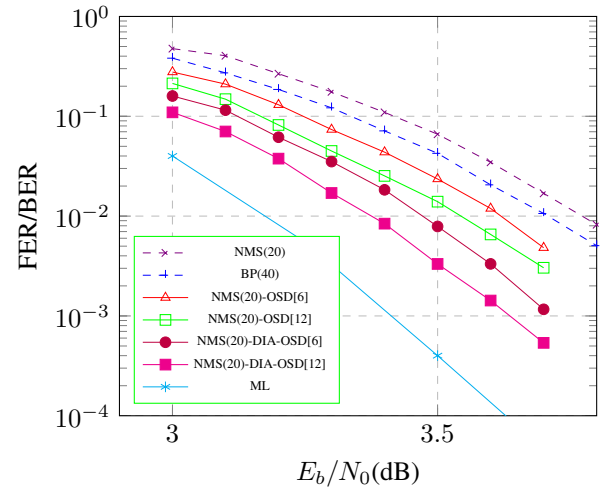


Fig. 6. Performance comparison for various decoding schemes of (1056,880) code

For Code B of longer block length, decoding enhancement becomes more challenging due to more classes of order patterns of higher order sum is solicited by OSD to attain targeted decoding performance, attributed to more scattered underlining order patterns. As shown in Fig.6, compared with NMS of $I_m = 20$ which is also compressed for the consideration of complexity like Code A, conventional BP of $I_m = 40$ leads only about 0.1 dB, and its advantage is reversed when the NMS equipped with OSD of $P_l = 6$. OSD of $P_l = 12$ yields another 0.1 dB gain at the cost of more computational complexity. Notably, the integration of DIA assists OSD of $P_l = 6$ to outperform $P_l = 12$ without DIA, but falls behind about 0.1 dB when DIA is presented. Regrettably, the computational complexity will be soaring with increased P_l , which will be elaborated in the next section. As a side note, existing feasible SOTA decoders which approach ML performance are confined to be applied for codes of short block length around one or two hundred, their scalability to longer block length remains to be investigated in future.

E. Complexity analysis

Since real addition and multiplication dominate most complexity of various decoders, we take into account their counts in complexity comparison hereafter, while selectively ignoring volumes of logical 'xor' or 'and' operations involved in the steps such as Gaussian elimination or candidate codeword generating, which is essentially hardware friendly.

The total complexity of proposed NMS-AID-OSD comprises computation occurred in triple constituent phases separately, among which NMS is one of the simplest MS variant with a single trainable parameter, AID is fulfilled via a three-layer CNN model, and OSD is implemented via following the predefined decoding path, whose length can be adjusted flexibly depending on applications.

The merit of choosing a specific decoding path for an OSD, instead of the conventional order-p in the literature, is

cleared via the comparison of trade-off between decoding and complexity. For instance of Code A, given the segmenting of its MRB delimited as $[0 \cdots 20 \cdots 40 \cdots 64]$, as observed in Table.II, the first 19 order-patterns occupies 33792 counts among total 33807 decoding failures. Such a dominance implies other patterns excluded from the list will contribute little to performance. Assuming a conventional order-4 OSD is equipped with DIA, then it will cover the leading 19 members in the list due to their order sum is less than or equal to 4, in addition to a handful of missed outliers. To benchmark it, an order-3 OSD will exclude some dominant patterns such as $[3,10],[4,0,0],[2,2,0]$ from the list. As a result, compared with conventional order-3,4 OSD, despite the extra minor benefits attributed to its outliers, we can safely declare the performance of OSD(12) and OSD(19), following the designated decoding path, are close to their performance respectively.

However, it tells another story in terms of computation complexity. Keeping in mind an error pattern of MRB will be mapped to one item in the candidate codeword list, and the criterion 6 of picking the best among them requires a full traversing through the list, commonly entailed with volumes of real additions, thus a desirable candidate codeword list will be sufficiently short but retains the authentic codeword as possible, which underlies the motivation of our decoding path design to substitute for the conventional order-p OSD. For Code A at SNR=3.0 dB, as indicated in Table.II, the accumulated count sum of all error patterns belonging to OSD(12) and OSD(19) is 10545 and 180790 according to

$$\sum_{l=1}^{P_l} \sum_{t_1=0}^{a^{(l)}} \sum_{t_2=0}^{b^{(l)}} \sum_{t_3=0}^{c^{(l)}} \binom{\lambda_1}{t_1} \binom{\lambda_2}{t_2} \binom{\lambda_3}{t_3}$$

where $\sum_{i=1}^3 \lambda_i = K$. While it reaches 43745 and 679121 for a conventional order-p=3,4 OSD respectively, which is evaluated via $\sum_{i=1}^p \binom{K}{i}$ at the MRB length $K = 64$. Therefore, at a cost of negligible performance loss, the adoption of our decoding path design saves nearly 3/4 the search work of conventional order-p OSD. Hence, the dual pros of saving memory and computation present convincing evidence to support our decoding path setting.

Compared with Code A, a similar observation can be drawn for Code B, although the workload grows considerably more heavy. With the MRB segmentation setting $[0 \cdots 40 \cdots 120 \cdots 880]$, it is found more order pattern types emerge beyond the 32 dominant ones listed in Table.II, leading to the ratio drops to $6135/6199 = 0.9896$. Even more, the fact some order patterns with order sum as high as 5 exists in the 32 dominant order patterns, pushes us to deliberately skip them when choosing a feasible decoding path with constrained complexity, but at the cost of performance penalty. To manage well the trade-off between performance and complexity, $P_l=12$, instead of 32, is chosen for the decoding path length in the simulation.

F. Complexity comparison with the SOTA decoder

For Code A, the proposed NMS-DIA-OSD(12) presented a similar decoding performance to the SOTA decoder of D_{10} -

OSD-2(25) [24] in the literature. It is thus meaningful to compare them as well in terms of complexity, latency etc.. In training phase, the SOTA decoder has to find out the dominant absorbing sets of the code firstly, then a bunch of BP-RNN decoders, one to one mapped to the chosen absorbing set, totally 10240 weights [24] are to be trained to maximize decoding improvement effectively. In contrast to that, our solution requires one single weight of NMS and another 313 weights belonging to CNN to be trained, resulting in a vastly relieved training overhead. Due to the weight count is perfectly indicative of complexity, the combination of NMS-DIA will thus be much less intensive compared to BP-RNN in terms of computational complexity. On the other hand, for the SOTA decoder, the OSD-2 element is invoked several times after each say 10 BP-RNN iterations, its diminishing complexity over the order sum 3 of our decoder patterns is largely cancelled out. Lastly, with the fact that quicker response of CNN over RNN, less I_m setting of NMS over BP, and one decoding call following the decoding path versus many calls of tradition OSD-2, it can be readily inferred our streamlined NMS-DIA-OSD(12) architecture has much higher throughput, or less latency over the SOTA decoder.

V. CONCLUSIONS AND FUTURE RESEARCH

To postprocess the decoding failures of NMS, the joint forces of bit-oriented deep learning based methods and word-oriented adapted OSD was employed to tackle them so as to boost the decoding performance of short to moderate LDPC codes to near ML decoding. Based on the suggested novel reliability metric and new decoding path configure for conventional OSD, our streamlined NMS-DIA-OSD solution was verified to outperform its counterparts in terms of decoding performance, high throughput, low complexity, and low latency.

It is worth of further study what is the optimal partition of the MRB bits, on which the order pattern layout relies heavily. Additionally, how to adjust it with varied block length remains to be investigated.

Instead of the CNN in use, there are more advanced NN structures available to be potential candidates of implementing DIA, which may result in a better reliability metric, thus facilitating the succeeded OSD to elevate decoding level. Actually, any scheme applicable for time series prediction is worth trying for the purpose of constructing new metrics. Furthermore, it is possible to utilize the decoder diversity by ensembling several DIA candidates for the OSD to pick the best codeword estimate via majority voting.

AVAILABILITY OF DATA

Parity check-matrices of Code A and Code B, as well as BP and ML decoding results can be retrieved at the website [20], thanks to the generosity of the original authors and great efforts taken for its maintenance.

ACKNOWLEDGMENT

The authors would like to thank Google corporation for providing the excellent computing platforms of Colab and

Kaggle online, which make it possible to debug, train and test our models freely. Thanks also are given to the anonymous reviewers for providing their valuable feedback in improving the quality of this paper.

REFERENCES

- [1] Robert Gallager. Low-density parity-check codes. *IRE Transactions on information theory*, 8(1):21–28, 1962.
- [2] David JC MacKay and Radford M Neal. Near shannon limit performance of low density parity check codes. *Electronics letters*, 32(18):1645, 1996.
- [3] Jianguang Zhao, Farhad Zarkeshvari, and Amir H Banihashemi. On implementation of min-sum algorithm and its modifications for decoding low-density parity-check (ldpc) codes. *IEEE transactions on communications*, 53(4):549–554, 2005.
- [4] Ming Jiang, Chunming Zhao, Li Zhang, and Enyang Xu. Adaptive offset min-sum algorithm for low-density parity check codes. *IEEE communications letters*, 10(6):483–485, 2006.
- [5] Marc PC Fossorier and Shu Lin. Soft-decision decoding of linear block codes based on ordered statistics. *IEEE Transactions on Information Theory*, 41(5):1379–1396, 1995.
- [6] Marc PC Fossorier, Miodrag Mihaljevic, and Hideki Imai. Reduced complexity iterative decoding of low-density parity check codes based on belief propagation. *IEEE Transactions on communications*, 47(5):673–680, 1999.
- [7] Marc PC Fossorier. Iterative reliability-based decoding of low-density parity check codes. *IEEE Journal on selected Areas in Communications*, 19(5):908–917, 2001.
- [8] Chentao Yue, Mahyar Shirvanimoghaddam, Giyoon Park, Ok-Sun Park, Branka Vucetic, and Yonghui Li. Probability-based ordered-statistics decoding for short block codes. *IEEE Communications Letters*, 25(6):1791–1795, 2021.
- [9] Chentao Yue, Mahyar Shirvanimoghaddam, Branka Vucetic, and Yonghui Li. Ordered-statistics decoding with adaptive gaussian elimination reduction for short codes. In *2022 IEEE Globecom Workshops (GC Wkshps)*, pages 492–497. IEEE, 2022.
- [10] Muhammad Imran Razzak, Saeeda Naz, and Ahmad Zaib. Deep learning for medical image processing: Overview, challenges and the future. *Classification in BioApps*, pages 323–350, 2018.
- [11] Tom Young, Devamanyu Hazarika, Soujanya Poria, and Erik Cambria. Recent trends in deep learning based natural language processing. *IEEE Computational intelligence magazine*, 13(3):55–75, 2018.
- [12] Sorin Grigorescu, Bogdan Trasnea, Tiberiu Cocias, and Gigel Macesanu. A survey of deep learning techniques for autonomous driving. *Journal of Field Robotics*, 37(3):362–386, 2020.
- [13] Eliya Nachmani, Yair Be’ery, and David Burshtein. Learning to decode linear codes using deep learning. In *2016 54th Annual Allerton Conference on Communication, Control, and Computing (Allerton)*, pages 341–346. IEEE, 2016.
- [14] Tobias Gruber, Sebastian Cammerer, Jakob Hoydis, and Stephan ten Brink. On deep learning-based channel decoding. In *2017 51st Annual Conference on Information Sciences and Systems (CISS)*, pages 1–6. IEEE, 2017.
- [15] Eliya Nachmani, Elad Marciano, Loren Lugosch, Warren J Gross, David Burshtein, and Yair Beery. Deep learning methods for improved decoding of linear codes. *IEEE Journal of Selected Topics in Signal Processing*, 12(1):119–131, 2018.
- [16] Fei Liang, Cong Shen, and Feng Wu. An iterative bp-cnn architecture for channel decoding. *IEEE Journal of Selected Topics in Signal Processing*, 12(1):144–159, 2018.
- [17] Loren Lugosch and Warren J Gross. Learning from the syndrome. In *2018 52nd Asilomar Conference on Signals, Systems, and Computers*, pages 594–598. IEEE, 2018.
- [18] Loren Peter Lugosch. *Learning algorithms for error correction*. McGill University (Canada), 2018.
- [19] Qing Wang, Shunfu Wang, Haoyu Fang, Leian Chen, Luyong Chen, and Yuzhang Guo. A model-driven deep learning method for normalized min-sum ldpc decoding. In *2020 IEEE International Conference on Communications Workshops (ICC Workshops)*, pages 1–6. IEEE, 2020.
- [20] Michael Helmling, Stefan Scholl, Florian Gensheimer, Tobias Dietz, Kira Kraft, Stefan Ruzika, and Norbert Wehn. Database of Channel Codes and ML Simulation Results. www.uni-kl.de/channel-codes, 2019.
- [21] Eliya Nachmani and Yair Beery. Neural decoding with optimization of node activations. *IEEE Communications Letters*, 2022.
- [22] Andreas Buchberger, Christian Hger, Henry D Pfister, Laurent Schmalen, and Alexandre Graell i Amat. Pruning and quantizing neural belief propagation decoders. *IEEE Journal on Selected Areas in Communications*, 39(7):1957–1966, 2020.
- [23] Andreas Buchberger, Christian Hger, Henry D Pfister, Laurent Schmalen, and Alexandre Graell i Amat. Learned decimation for neural belief propagation decoders. In *ICASSP 2021-2021 IEEE International Conference on Acoustics, Speech and Signal Processing (ICASSP)*, pages 8273–8277. IEEE, 2021.
- [24] Joachim Rosseel, Valrian Mannoni, Inbar Fijalkow, and Valentin Savin. Decoding short ldpc codes via bp-rnn diversity and reliability-based post-processing. *IEEE Transactions on Communications*, 70(12):7830–7842, 2022.
- [25] Orange Book. *Short Blocklength LDPC codes for TC synchronization and channel coding*. Orange, 2012.
- [26] Michael Helmling, Stefan Scholl, Florian Gensheimer, Tobias Dietz, Kira Kraft, Stefan Ruzika, and Norbert Wehn. Database of Channel Codes and ML Simulation Results. www.uni-kl.de/channel-codes, 2019.